ISBN: 978-3-95450-214-1 ISSN: 2673-5490 doi:10.18429/JACoW-IPAC2021-TUXB04

# FABRICATION AND TUNING OF A THz-DRIVEN ELECTRON GUN

S. M. Lewis*[1], A. Haase, J. Merrick, E. A. Nanni, M. Othman, S. Tantawi
SLAC National Accelerator Laboratory, Menlo Park, USA
[1]now at Fermi National Accelerator Laboratory, Batavia, USA

*Abstract*

We have developed a THz-driven field emission electron gun and beam characterization assembly. The two cell standing-wave gun operates in the $\pi$ mode at 110.08 GHz. It is designed to produce 360 keV electrons with 500 kW of input power supplied by a 110 GHz gyrotron. Multiple gun structures were electroformed in copper using a high precision diamond-turned mandrel. The field emission cathode is a rounded copper tip located in the first cell. The cavity resonances were mechanically tuned using azimuthal compression. This work will discuss details of the fabrication and tuning and present the results of low power measurements.

## INTRODUCTION

Across the accelerator community, there is demand for new electron source technology [1]. Plans for future Free Electron Laser (FEL) and Ultrafast Electron Diffraction (UED) facilities aim for improvements in beam emittance, brightness, bunch length, and energy spread. All of these parameters are heavily influenced by the electron source.

In RF cavity-based electron sources, significant improvements can be made by accelerating electrons with high gradients. This helps preserve the beam quality while limiting the complexity and footprint of the accelerator structure. Vacuum breakdown limits the achievable gradient in normal conducting RF (NCRF) structures. Studies of breakdown behavior have shown that high fields can be achieved in higher frequency cavities [2–5]. Experiments in normal conducting copper structures at 110 GHz have demonstrated this scaling, reaching gradients as high as 230 MV/m with peak surface electric fields up to 520 MV/m [6]. In these experiments, the achieved maximum gradient was limited only by the available source power.

The high surface fields provide an opportunity to develop an electron source based on field emission. Most electron guns currently in use are photocathodes, which use a laser to produce the beam and cavities for acceleration. With high enough RF fields within the cavity, emission can occur due to the surface field without an additional excitation. This phenomenon is known as cold field emission and is described by the Fowler-Nordheim equation [7]. This method provides natural synchronization between the electron bunch production and the RF cycles and only requires one source to supply RF power. In THz cavities, the sustainable peak surface fields are high enough that field emission can occur on a copper cathode shaped to provide local field enhancement.

Much of the challenge of developing THz cavities lies in the fabrication of the mm-scale structures. However, advances in machining and additive manufacturing techniques makes it possible to reliably build THz frequency structures. Previous work has demonstrated the capabilities of CNC machining of copper THz structures [8, 9]. In this work, we present details of the design and performance of a 110 GHz electron gun fabricated using diamond turning and electroforming. This technique is capable of producing cavities in one continuous piece, which allows for successful mechanical tuning through compression.

## DESIGN AND MODELLING

The electron gun is designed as a 2 cell standing wave gun operating in the $\pi$ mode at 110 GHz. A copper tip with a 50 µm radius of curvature located in the center of the first cell serves as the field emission source. This tip provides a field enhancement of 4.5 times the highest surface field elsewhere in the structure. A schematic of the design in shown in Fig. 1a and dimensions of the structure are listed in Table 1. Power is coupled into the structure on-axis through a circular waveguide. This gun was designed to utilize a Gaussian horn and mode converter structure that was developed for previous W-band tests [10, 11]. Simulated fields inside the gun and mode converter are shown in Fig. 1b.

Table 1: Design Values of the Copper Tip Gun

| Parameter | Value (mm) | Description |
|---|---|---|
| a | 0.286 | Iris radius |
| ac | 0.408 | Coupling iris radius |
| b1 | 1.080 | Radius of first cell |
| b2 | 1.155 | Radius of second cell |
| bc | 1.185 | Radius of input waveguide |
| p1 | 0.51 | Length of first cell |
| p2 | 0.51 | Length of second cell |
| ri | 0.1 | Iris radius of curvature |
| tf | 0.1 | Tip base radius of curvature |
| tl | 0.255 | Tip length |
| tr | 0.050 | Tip radius of curvature |

The structure was optimized for 500 kW of input power from a 110 GHz gyrotron source [12, 13]. To determine the acceleration performance, the full complex 3D fields were exported from HFSS, scaled to the appropriate input power, and used as an input to model the beam in GPT [14, 15]. Over the 1.6 mm length of the structure, the bunch is accelerated to $\gamma = 1.71$–$1.72$, or about 365 keV [16]. The field emission behavior was modeled by applying the Fowler-Nordheim

* smlewis@slac.stanford.edu

ISBN: 978-3-95450-214-1 ISSN: 2673-5490 doi:10.18429/JACoW-IPAC2021-TUXB04



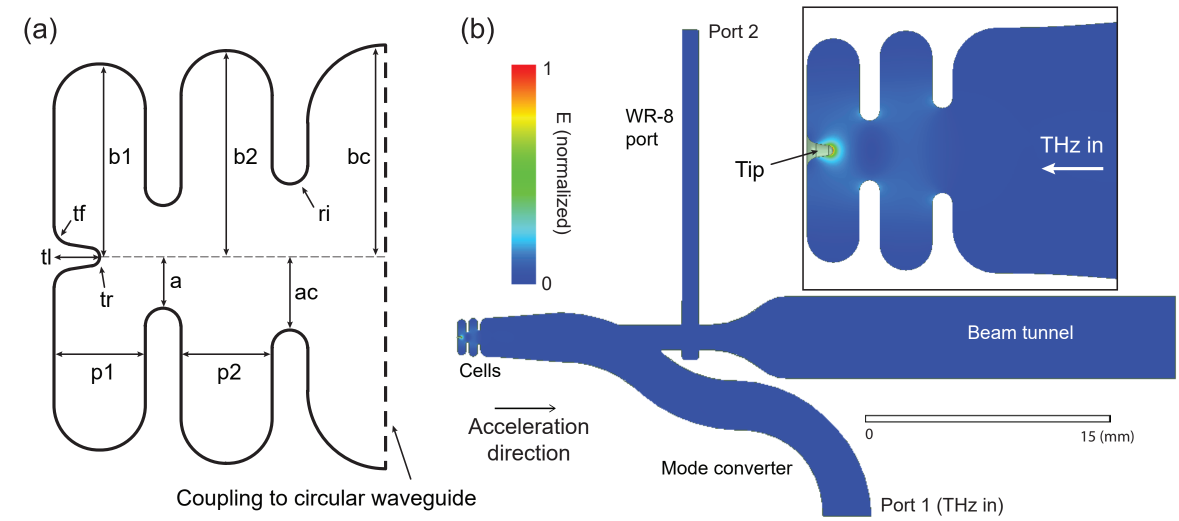


Figure 1: (a) Schematic of the gun cells and tip. The structure is cylindrically symmetric around the horizontal dashed line. The design values of the indicated parameters are listed in Table 1. Power is coupled into the cells through a circular wageuide (vertical dashed line). (b) Electric field magnitude in the vacuum space of the gun and mode converter at the $\pi$ mode resonance. The simulation uses copper surface resistivity on the structure walls and assumes mirror symmetry. The inset shows a closer view of the fields in the cells and around the tip.

equation at discrete points along the cathode tip surface using the HFSS fields. This method gives an estimate of 51.3 fC per bunch for 500 kW of input power [16].

## FABRICATION

Cavities with similar geometry to the gun cells have been previously fabricated through CNC machining [8, 9]. The size and location of the copper tip adds an additional challenge. The gun was designed to be fabricated using electroforming, which allows the tip and cells to be made in one piece. The vacuum space of the cavities was machined into an aluminum mandrel using diamond turning. The tip geometry was removed from the mandrel using wire EDM. Copper was electroformed around the mandrel, forming the tip and cavity walls. Finally, the aluminum mandrel was removed using chemical processing.

Eight structures were fabricated in one batch. Photos and microscope images of the structures are shown in Fig 2. Based on measurements using a laser confocal microscope, the dimensions of the visible features match well with the design. Figure 3 shows 3D data of the copper tip profile which demonstrate the high precision of the diamond turning and electroforming processes. The eight structures showed some variation in the surface finish and sizes of the irises. Some pitting is also visible, which is likely a result of chemical processing of the mandrel. Additional work was performed to study plating and etching of the finished structures. Full details of these studies can be found in [16].

## COLD TESTING AND TUNING

Cold tests were performed to measure the resonances of the eight structures. In each structure, both the o mode and $\pi$ mode were visible. The two modes were lower in frequency than the design values of 109.22 GHz and 110.01 GHz respectively. Across the eight structures, the range of measured frequencies was 108.17–108.54 GHz for the o mode and 109.61–109.9 GHz for the $\pi$ mode. There was a noticeable difference in the mode spacing and relative strength compared to the design simulations. Some improvement was achieved with HCl etching, indicating that some residual material from the mandrel may have been partially responsible for the shift [16].

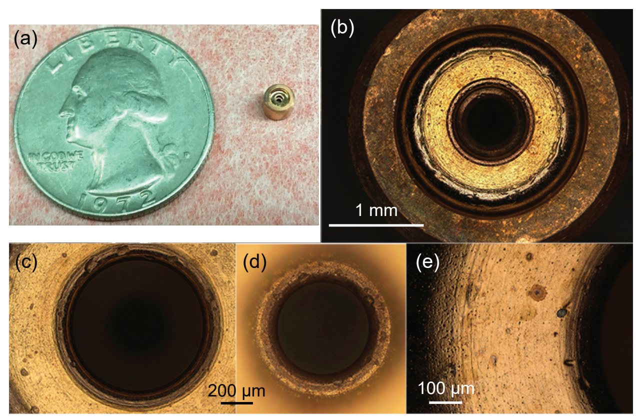


Figure 2: (a) Photo of a fabricated gun structure. (b-e) Focus stacked microscope images of (b) a gun structure looking through the circular waveguide opening, (c) the coupling iris, (d) the iris between the two cells, and (e) a close-up of the edge and surface of a coupling iris.

The highest performing range of the gyrotron source is 110.08–110.1 GHz, and thus it was necessary to tune the structures. Some tuning could be achieved by cooling the

ISBN: 978-3-95450-214-1 ISSN: 2673-5490 doi:10.18429/JACoW-IPAC2021-TUXB04

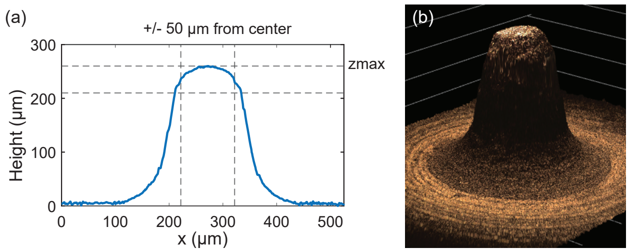


Figure 3: Example 3D measurements of the tip profile taken on a laser confocal microscope. (a) The height data versus lateral position. The dashed lines indicate the maximum height and ±50 µm from the top and center. The tip was designed to have a height of 255 µm and a 50 µm radius of curvature. (b) A 3D view of tip height data.

structures, but not enough to bring any within the source range. Mechanical tuning of W-band cavities is extremely challenging due to their small size. The unique geometry of the cylindrical electroformed structures provided a new opportunity to attempt tuning through azimuthal compression.

After cleaning with an HCl etch, several structures were tuned using a collet to perform the compression, shown in Fig. 4. Due to uneven compression depending on the orientation of the structure, it was possible to intentionally tune the o mode by a greater amount than the $\pi$ mode, bringing the structure closer to its design field balance. Figure 5 shows the results of tuning for one structure. The o mode was tuned from 108.555 GHz to 109.332 GHz (777 MHz shift) and the $\pi$ mode was tuned from 109.911 GHz to 110.081 GHz (170 MHz shift). Measurements were performed throughout the tuning process showing the achievable steps, Fig. 5b. No additional shifts were observed in repeated measurements weeks after the initial tuning, indicating that the tuning is permanent. The resonances also remained consistent cycling from air to vacuum. This gun was incorporated into the full gun assembly for high power testing [11, 16].

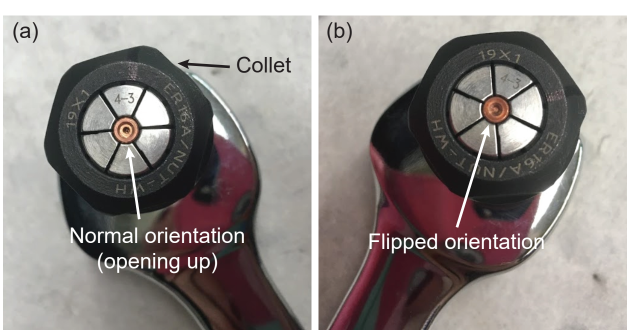


Figure 4: Images of a gun structure in the collet used for tuning. The compression is not perfectly even, so two orientations were used for tuning: (a) shows the 'normal' orientation with the waveguide opening pointing up, and (b) shows the 'flipped' orientation.

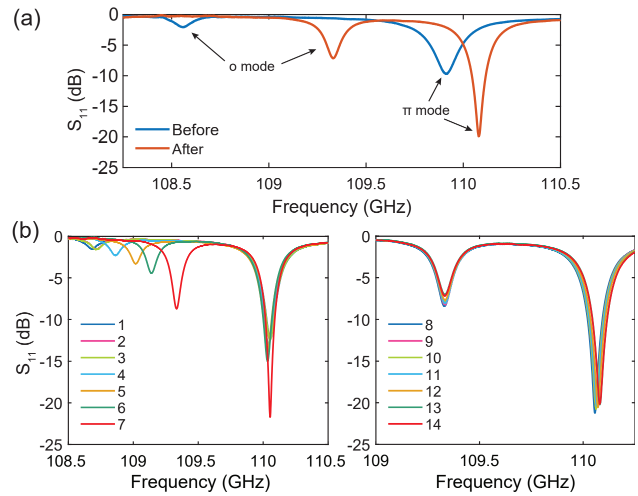


Figure 5: (a) Measured modes before and after tuning. The o mode and $\pi$ mode (indicated) were intentionally tuned by different amounts. Interim measurements taken throughout the tuning are shown in (b). Measurements in the left plot show the tuning of primarily the o mode, which correspond to the 'normal' orientation shown in Fig. 4a. The right plot shows the fine tuning of the $\pi$ mode using the 'flipped' orientation, Fig. 4b. The labels of the measurements correspond to the order in which they were performed.

## CONCLUSION

High frequency NCRF cavities are a promising technology for future compact, high gradient accelerators. We have developed a field emission electron gun based on W-band cavities to utilize advances in manufacturing technology. We have demonstrated the feasibility of using electroforming to fabricate complex W-band structures with high precision. The cavities can be tuned mechanically, which is an important requirement for practical high frequency accelerators.

The electron gun will now be tested with high power, building on previous breakdown studies. The goal of these measurements will be to characterize the resulting beam, particularly the energy spread, charge, and size. This will serve as a new regime of study for field emission behavior due to the very high surface fields in the structure. Full details of the gun development and high power testing will be presented in a future paper.

## ACKNOWLEDGMENTS

The authors would like to thank the engineers, technicians, and staff from the SLAC TID Advanced Prototyping and Fabrication department. This work was supported by the Department of Energy Contract No. DE-AC02-76SF00515 (SLAC) and by NSF Grant No. PHY-1734015.

## REFERENCES

[1] X. Wang, P. Musumeci, E. Lessner, and J. Goldstein, "Report of the Basic Energy Sciences Workshop on the Future of Electron Sources", Department of Energy, United States, Rep. OSTI-1616511, 2016. doi:10.2172/1616511

ISBN: 978-3-95450-214-1 ISSN: 2673-5490 doi:10.18429/JACoW-IPAC2021-TUXB04


[2] C. Limborg *et al.*, "Performance of a first generation X-band photoelectron rf gun", *Phys. Rev. Accel. Beams*, vol. 19, p. 053401, May. 2016. doi:10.1103/PhysRevAccelBeams.19.053401

[3] M. Dal Forno *et al.*, "rf breakdown tests of mm-wave metallic accelerating structures", *Phys. Rev. Accel. Beams*, vol. 19, p. 011301, Jan. 2016. doi:10.1103/PhysRevAccelBeams.19.011301

[4] J. A. Rodriguez *et al.*, "30 GHz High-Gradient Accelerating Structure Test Results", in *Proc. PAC'07*, Albuquerque, NM, USA, Jun. 2007, paper FROBC01, pp. 3818–3820.

[5] W. Wuensch *et al.*, "High-gradient Test Results from a CLIC Prototype Accelerating Structure: TD26CC", in *Proc. IPAC'14*, Dresden, Germany, Jun. 2014, pp. 2285–2287. doi:10.18429/JACoW-IPAC2014-WEPME015

[6] M. A. K. Othman *et al.*, "Experimental demonstration of externally driven millimeter-wave particle accelerator structure," *Appl. Phys. Lett.*, vol. 117, p. 073502, 2020. doi:10.1063/5.0011397

[7] R. H. Fowler and L. Nordheim, "Electron emission in intense electric fields", *Proc. R. Soc. Lond. A*, vol. 119, pp. 117–181, 1928. doi:10.1098/rspa.1928.0091

[8] E. A. Nanni *et al.*, "Prototyping High-Gradient mm-Wave Accelerating Structures", in *Proc. IPAC'17*, Copenhagen, Denmark, May 2017, pp. 2902–2905. doi:10.18429/JACoW-IPAC2017-WEPAB138

[9] M. A. K. Othman *et al.*, "Prototyping of Brazed mm-Wave Accelerating Structures", in *Proc. IPAC'19*, Melbourne, Australia, May 2019, pp. 3764–3765. doi:10.18429/JACoW-IPAC2019-THPGW078

[10] E. A. Nanni *et al.*, "Toward High-Power High-Gradient Testing of mm-Wave Standing-Wave Accelerating Structures", in *Proc. IPAC'18*, Vancouver, Canada, Apr.-May 2018, pp. 1224–1227. doi:10.18429/JACoW-IPAC2018-TUZGBE4

[11] S. M. Lewis *et al.*, "A THz-driven field emission electron gun", in *Proc. IRMMW-THz'20*, Buffalo, United States, Nov. 2020, pp. 1–2. doi:10.1109/IRMMW-THz46771.2020.9370485

[12] D. Tax, "Experimental study of a high efficiency step-tunable MW gyrotron oscillator", Ph.D. thesis, Massachusetts Institute of Technology, United States, 2013.

[13] J. Genoud *et al.*, "Study of the effect of reflections on high-power 110-GHz pulsed gyrotron operation", *J. Infrared Milli. Terahz. Waves*, vol. 42, p. 557, 2021. doi:10.1007/s10762-021-00769-8

[14] Ansys, Ansys HFSS: High Frequency Electromagnetic Field Simulation, https://www.ansys.com/products/electronics/ansys-hfss

[15] S. B. van der Greer and M. J. de Loos, General Particle Tracer, http://www.pulsar.nl/gpt/.

[16] S. M. Lewis, "A THz-driven electron gun", Ph.D. thesis, University of California, Berkeley, United States, 2020.